High Throughput Screening of M_3C_2 MXenes for Efficient CO_2 Reduction Conversion into Hydrocarbon Fuels

Yi Xiao [a*], Weibin Zhang [b]

[a] Institute of Materials Science, TU Darmstadt, 64287 Darmstadt, Germany

[b] School of Physics and Optoelectronic Engineering, Yangtze University, Jingzhou, 434023, P. R. China

E-mail addresses: yixiao@tmm.tu-darmstadt.de;

THERMOCHEMISTRY ANALYSIS

The fundamental thermodynamic equation defined as follow:

$$G = H - TS \quad (1)$$

Under the standard DFT calculation conditions (T = 0 K), so the TS is almost negligible. Actually, when the temperatures greater than 0 K and constant pressure, that means normal temperature and pressure conditions (here T = 298.15 K), zero point energy (ZPE) corrections can be included to finally obtain, enthalpy for a given temperature can be expressed in terms of

$$G=H^0+\text{ZPE-T}S \quad (2)$$

In addition, the entropy term can be calculated as the sum of the translational, rotational, vibrational, and electronic contributions as to:

$$S=S_t+S_r+S_v+S_e \quad (3)$$

and also, the total corrections can be included to finally obtain:

$$G=H_0+\text{ZPE-T}(S_t+S_r+S_v+S_e) \quad (4)$$

When computing the change of Gibbs free energy variation between two different states named a and b by applied eqn. (4), So ΔG results in:

$$\Delta G = H_b^0 + ZPE_b - T(S_{t,b} + S_{r,b} + S_{v,b} + S_{e,b}) - H_a^0 + ZPE_a - T(S_{t,a} + S_{r,a} + S_{v,a} + S_{e,a}) \quad (5)$$

Or simply format:

$$\Delta G = \Delta H_{ba}^0 + \Delta ZPE_{ba} - T\Delta S_{ba} \quad (6)$$

$$\Delta\text{G}(298.15\,\text{K}) = \Delta\text{E}_{\text{DFT}} + \Delta\text{ZPE} + \Delta\text{H(T)} - \text{TS(T)} \quad (7)$$

$$\Delta H(T) = H(T) - H(0) = \int_0^T C_p dT \quad (8)$$

$$\Delta\text{ZPE} = 1/2\text{h}\nu \quad (9)$$

$$S(\text{T}) = S_t + S_r + S_v + S_e \quad (10)$$

$$H(T) = H(0) + PV \quad (11)$$

For the last equation, there are some approximations can be applied for entropy as reported in ref. 1 and ref. 2 (see Supporting Information).

1. At the fundamental electronic level: $S_e \approx 0$
2. For gases, translational, rotational, and vibrational entropy terms have contributions that might not be neglected, and therefore: $S = S_t + S_r + S_v$
3. For solids and adsorbates, both $S_t \approx 0$ and $S_r \approx 0$, and therefore: $S = S_v$

Since these thermal corrections for the enthalpy have been taken into account for the ΔG calculation.

$\eta=U_0-U$ is the overpotential. In other words, adsorbed hydrocarbon and hydroxide on the MXene catalysts surface are thermodynamic for the oxygen reduction process, and the activation energy for the total process at the maximum cell voltage U_0 0.17 V is at least ΔG= -1.35 eV. This value is, indeed, close to the experimentally observed over potential.

Table S1. Schematic energy profiles for the CO_2RR for all the favorable pathways on Mo_3C_2 surface. (b) Pathway 2, (c) Pathway 3, and (d) Pathway 4 on M_3C_2 surface. The corresponding formula with Gibbs free energy change is shown in eV. Blue and black texts represent spontaneous and nonspontaneous reactions (in eV), respectively (bottom).

System	$U_L(CO_2)$	$UL(H_2)$	$U_L(CO_2)$-$U_L(H_2)$	System	$U_L(CO_2)$	$U_L(H_2)$	$U_L(CO_2)$-$U_L(H_2)$
Sc_3C_2	-2.63	0.13	-2.76	Nb_3C_2	-0.51	-1.12	0.61
Ti_3C_2	-0.01	0.04	-0.05	Mo_3C_2	-0.91	-0.34	-0.57
V_3C_2	-0.47	-0.08	-0.39	Mo_2TiC_2	0.49	-0.21	0.70
Cr_3C_2	-0.24	-0.46	0.23	Hf_3C_2	-2.86	-0.87	-1.99
Y_3C_2	-1.99	0.42	-2.40	Ta_3C_2	0.00	0.04	-0.04
Zr_3C_2	-2.73	-1.11	-1.62	W_3C_2	0.66	-0.52	1.18

Table S2. Zero-point energy (ZPE, in eV) and entropy corrections (TS, in eV) at T = 298 K for gas and liquid phase molecules and adsorbed species.The unit for energy is eV. Intermediates species of energy profiles for the CO_2RR for all the favorable pathways on M_3C_2 surface.

Species	**ΔZEP**	**ΔU(T)**	**ΔH(T)**	**ΔG(T)**	**T×ΔS**
CO_2	0.306911	0.379147	0.404839	-0.303304	0.708143
HCO_2	0.538326	0.621134	0.646826	-0.150702	0.797528
H_2CO_2	0.592443	0.708158	0.73385	-0.211201	0.945051
H_2COOH	1.076272	1.178516	1.204208	0.335541	0.868667
H_2CO	0.704777	0.783085	0.808777	0.079215	0.729562
H_3CO	0.938608	1.020442	1.046134	0.296878	0.749256
O	0.000132	0.038538	0.06423	-0.396455	0.460685
OH	0.240325	0.304554	0.330246	-0.229766	0.560012
H_2O	0.572122	0.649304	0.674996	0.050668	0.624328
COOH	0.52972	0.621317	0.647009	-0.173601	0.82061
HCOOH	0.824796	0.913339	0.939031	0.10034	0.838691
HCO	0.329327	0.408534	0.434226	-0.289523	0.723749
H_2COH	0.984677	1.079098	1.104789	0.313084	0.791705
H_3COH	1.344719	1.447594	1.473286	0.62377	0.849516
CH_3	0.801679	0.883117	0.908809	0.274153	0.634656
CH_4	0.974949	1.102064	1.127756	0.390872	0.736884
OOH	0.096632	0.160967	0.186659	-0.447249	0.633908
O_2	0.096632	0.160967	0.186659	-0.447249	0.633908
H_2	0.260748	0.324978	0.35067	-0.080206	0.430876
CO	0.172385	0.236615	0.262307	-0.375846	0.638153

Table S3. Zero-point energy (ZPE, in eV) and entropy corrections (TS, in eV) at T = 298 K for different slabs. The unit for energy is eV of reaction pathway followed for the CO_2 conversion mechanism into CH_4 catalyzed by M_3C_2.

MXene	Temperature	S (eV/K)	TΔS	ΔZPE	ΔH	ΔG
Cr_3C_2	298.15	0.0091	2.71452	2.63726	1.44383	1.36657
Hf_3C_2	298.15	0.01047	3.12196	2.92359	1.58317	1.3848
Mn_3C_2	298.15	0.00844	2.51732	2.57725	1.36245	1.42237
Mo_3C_2	298.15	0.00946	2.8194	2.14598	1.3967	0.72329
Mo_2TiC_2	298.15	0.00954	2.84379	2.83391	1.52667	1.51679
Nb_3C_2	298.15	0.00905	2.6987	2.92903	1.48513	1.71547
Sc_3C_2	298.15	0.0081	2.41425	2.44873	1.37661	1.41109
Ta_3C_2	298.15	0.01086	3.23681	2.80325	1.62938	1.19583
Ti_3C_2	298.15	0.0069	2.05705	3.38021	1.23947	2.56263
V_3C_2	298.15	0.00799	2.38314	3.11869	1.37204	2.10759
W_3C_2	298.15	0.0082	2.44585	1.88433	1.13679	0.57528
Y_3C_2	298.15	0.01111	3.31374	1.96627	1.6658	0.31832
Zr_3C_2	298.15	0.00939	2.80056	3.01031	1.47676	1.68651

Table S4. Gibbs free energies at 298.15 K by adding entropic (TS) and zero-point energy (ZPE) to the fluid phase molecules corrections to adsorbed species corrections applied), in eV, corresponding to the different intermediates along the CO_2 conversion pathway catalysed by M_3C_2 MXene.

Path1	MXene	Sc_3C_2	Ti_3C_2	V_3C_2	Cr_3C_2	Y_3C_2	Zr_3C_2	Nb_3C_2	Mo_3C_2	Mo_2TiC_2	Hf_3C_2	Ta_3C_2	W_3C_2
Surface	e^- transferred	0.00	0.00	0.00	0.00	0.00	0.00	0.00	0.00	0.00	0.00	0.00	0.00
CO_2	0	-2.63	-0.01	-0.47	-0.24	-1.99	-2.73	-0.51	-0.91	0.49	-2.86	0.00	0.66
HCO_2	1	-2.65	-2.45	-1.41	-4.54	-1.94	-2.15	-1.58	-0.91	-0.87	-2.00	-1.43	-0.74
H_2CO_2	2	-4.13	-3.74	-2.01	-4.23	-3.29	-3.65	-2.48	-1.14	-1.18	-3.59	-2.42	-1.05
H_2COOH	3	-2.55	-1.86	-1.42	-2.30	-2.00	-2.60	-1.38	-1.01	-0.84	-2.52	-1.44	-1.26
H_2CO	4	-0.73	-0.95	-0.80	-1.38	-0.40	-0.72	-0.84	-0.54	-0.57	-0.76	-1.03	-0.63
H_3CO	5	-3.76	-2.83	-2.19	-2.53	-3.20	-3.53	-2.37	-1.82	-1.64	-3.79	-2.49	-2.04
O	6	-4.96	-3.37	-3.16	-3.20	-4.34	-5.22	-3.23	-2.52	-2.08	-2.84	-3.44	-2.87
OH	7	-3.99	-3.96	-3.32	-3.60	-3.45	-3.75	-3.51	-3.03	-2.83	-3.79	-3.68	-3.25
H_2O	8	-3.12	-3.20	-3.16	-3.12	-2.88	-3.09	-3.18	-3.13	-3.12	-3.13	-3.27	-3.20
Path2	MXene	Sc_3C_2	Ti_3C_2	V_3C_2	Cr_3C_2	Y_3C_2	Zr_3C_2	Nb_3C_2	Mo_3C_2	Mo_2TiC_2	Hf_3C_2	Ta_3C_2	W_3C_2
Surface	e^- transferred	0.00	0.00	0.00	0.00	0.00	0.00	0.00	0.00	0.00	0.00	0.00	0.00
CO_2	0	-2.63	-0.01	-0.47	-0.24	-1.99	-2.73	-0.51	-0.91	0.49	-2.86	0.00	0.66
COOH	1	-0.17	-0.27	-0.35	-0.90	0.20	-0.83	-0.14	-0.43	-0.39	0.22	-0.77	-0.48
CO	2	-2.14	-2.32	-0.66	-3.47	-1.77	-2.13	-1.46	-0.53	-0.66	-2.39	-2.10	-0.89
CHO	3	-2.72	-1.94	-0.49	-1.27	-1.69	-1.45	-2.50	-1.09	-0.43	-3.50	-1.59	-1.20
H_2CO	4	-0.73	-0.95	-0.80	-1.38	-0.40	-0.72	-0.84	-0.54	-0.57	-0.76	-1.03	-0.63
H_2COH	5	-1.41	-1.43	-0.68	-1.54	-0.90	-1.11	-1.10	-0.89	-0.56	-1.02	-1.14	-1.05
H_3COH	6	-1.05	-1.11	-1.28	-1.88	-1.08	-1.16	-1.32	-1.20	-1.29	-1.16	-1.27	-1.09
CH_3	7	-1.80	-1.92	-1.86	-1.50	-1.47	-1.80	-1.76	-2.00	-1.78	-2.86	-1.86	-2.18
CH_4	8	-2.28	-2.34	-2.49	-2.48	-2.26	-2.22	-2.34	-2.44	-2.51	-2.21	-2.37	-1.49
Path3	MXene	Sc_3C_2	Ti_3C_2	V_3C_2	Cr_3C_2	Y_3C_2	Zr_3C_2	Nb_3C_2	Mo_3C_2	Mo_2TiC_2	Hf_3C_2	Ta_3C_2	W_3C_2

Surface	e- transferred	0.00	0.00	0.00	0.00	0.00	0.00	0.00	0.00	0.00	0.00	0.00	0.00
CO_2	0	-2.63	-0.01	-0.47	-0.24	-1.99	-2.73	-0.51	-0.91	0.49	-2.86	0.00	0.66
HCO_2	1	-2.65	-2.45	-1.41	-4.54	-1.94	-2.15	-1.58	-0.91	-0.87	-2.00	-1.43	-0.74
H_2CO_2	2	-4.13	-3.74	-2.01	-4.23	-3.29	-3.65	-2.48	-1.14	-1.18	-3.59	-2.42	-1.05
H_2COOH	3	-2.55	-1.86	-1.42	-2.30	-2.00	-2.60	-1.38	-1.01	-0.84	-2.52	-1.44	-1.26
H_2CO	4	-0.73	-0.95	-0.80	-1.38	-0.40	-0.72	-0.84	-0.54	-0.57	-0.76	-1.03	-0.63
H_3CO	5	-3.76	-2.83	-2.19	-2.53	-3.20	-3.53	-2.37	-1.82	-1.64	-3.79	-2.49	-2.04
H_3COH	6	-1.05	-1.11	-1.28	-1.88	-1.08	-1.16	-1.32	-1.20	-1.29	-1.16	-1.27	-1.09
CH_3	7	-1.80	-1.92	-1.86	-3.50	-1.47	-1.80	-1.76	-2.00	-1.78	-2.86	-1.86	-2.18
CH_4	8	-2.28	-2.34	-2.49	-2.48	-2.26	-2.22	-2.34	-2.44	-2.51	-2.21	-2.37	-1.49
Path4	MXene	Sc_3C_2	Ti_3C_2	V_3C_2	Cr_3C_2	Y_3C_2	Zr_3C_2	Nb_3C_2	Mo_3C_2	Mo_2TiC_2	Hf_3C_2	Ta_3C_2	W_3C_2
Surface	e- transferred	0.00	0.00	0.00	0.00	0.00	0.00	0.00	0.00	0.00	0.00	0.00	0.00
CO_2	0	-2.63	-0.01	-0.47	-0.24	-1.99	-2.73	-0.51	-0.91	0.49	-2.86	0.00	0.66
COOH	1	-0.17	-0.27	-0.35	-0.90	0.20	-0.83	-0.14	-0.43	-0.39	0.22	-0.77	-0.48
CO	2	-0.12	-0.85	-1.23	-1.52	0.18	-0.54	-1.13	-1.28	-1.49	-0.61	-1.37	-1.30
CHO	3	-2.72	-1.94	-0.49	-1.27	-1.69	-1.45	-2.50	-1.09	-0.43	-3.50	-1.59	-1.20
H_2CO	4	-0.73	-0.95	-0.80	-1.38	-0.40	-0.72	-0.84	-0.54	-0.57	-0.76	-1.03	-0.63
H_2COH	5	-1.41	-1.43	-0.68	-1.54	-0.90	-1.11	-1.10	-0.89	-0.56	-1.02	-1.14	-1.05
H_3COH	6	-1.05	-1.11	-1.28	-1.88	-1.08	-1.16	-1.32	-1.20	-1.29	-1.16	-1.27	-1.09
CH_3	7	-1.80	-1.92	-1.86	-3.50	-1.47	-1.80	-1.76	-2.00	-1.78	-2.86	-1.86	-2.18
CH_4	8	-2.28	-2.34	-2.49	-2.48	-2.26	-2.22	-2.34	-2.44	-2.51	-2.21	-2.37	-1.49

Table S5.Gibbs free energy and equilibrium potentials of several possible CO_2RR cathode reactions.

Cathode Reaction	ΔG(eV)	U_0 vs RHE(V)
$CO_2+2H^++2e^-\rightarrow CO(g)+H_2O$	0.21	-0.11
$CO_2+6H^++6e^-\rightarrow CH_3OH(l)+H_2O$	-0.10	0.02
$CO^2+8H^++8e^-\rightarrow CH_4(g)+2H_2O$	-1.35	0.17
$CO_2+2H^++2e^-\rightarrow HCOOH(l)+H_2O$	0.50	-0.25
$CO_2+4H^++4e^-\rightarrow HCHO(l)+H_2O$	0.28	-0.07

Gibbs free energy of reaction for CO_2RR elementary steps involving (H^++e^-) pair transfer was calculated using computational hydrogen electrode (CHE) model, it defined as ΔGn(U)=ΔG n(U=0) +neU, where n is the number of (H^++e^-) pairs transferred in CO_2RR and U is the electrode potential versus the reversible hydrogen electrode (RHE). ΔGpH represents the correction of the free energy due to the variations in H^+ concentration, defined as GpH=-kTln[H^+] = kTln10×pH, and the value of pH was set to 0 for strong acidic medium in this work and therefore, the calculated limiting potentials (U_L) were referenced to the RHE.

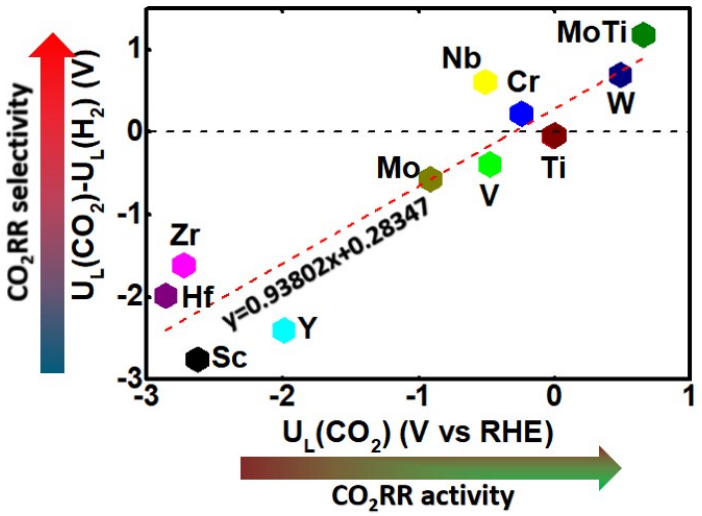

Figure. S1 Plot of $U_L(CO_2)$ -$U_L(H_2)$ as a function of U_L (CO_2) showing the selectivity of CO_2RR relative to HER for MXenes. Vertical line in (c) marks the equilibrium potential for the reduction of CO_2 to CH_4 (0.17 V vs. RHE).

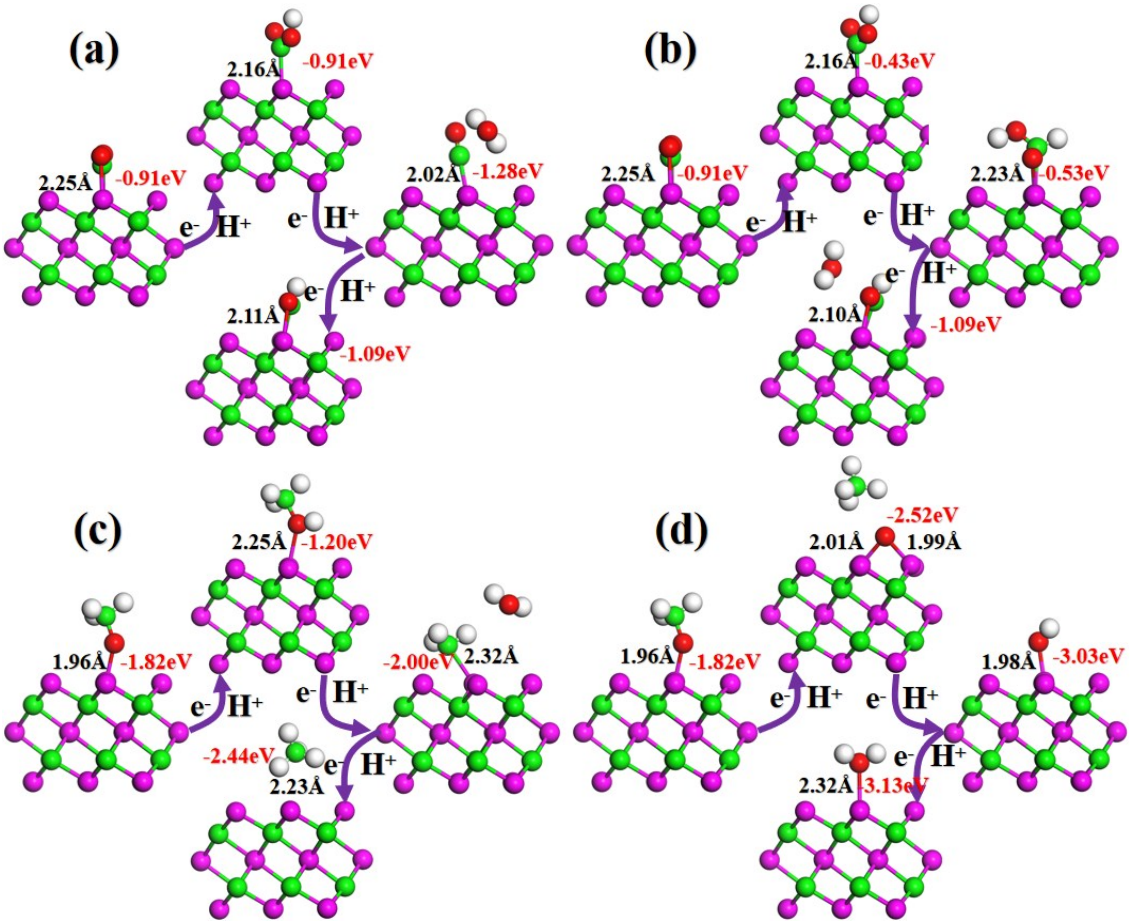

Figure.S2 (a) Scheme of a CO_2RR homogeneous electrocatalyst. b) Scheme of CO2RR heterogeneous electrocatalyst. c) Scheme of an immobilized catalyst for the CO2RR.

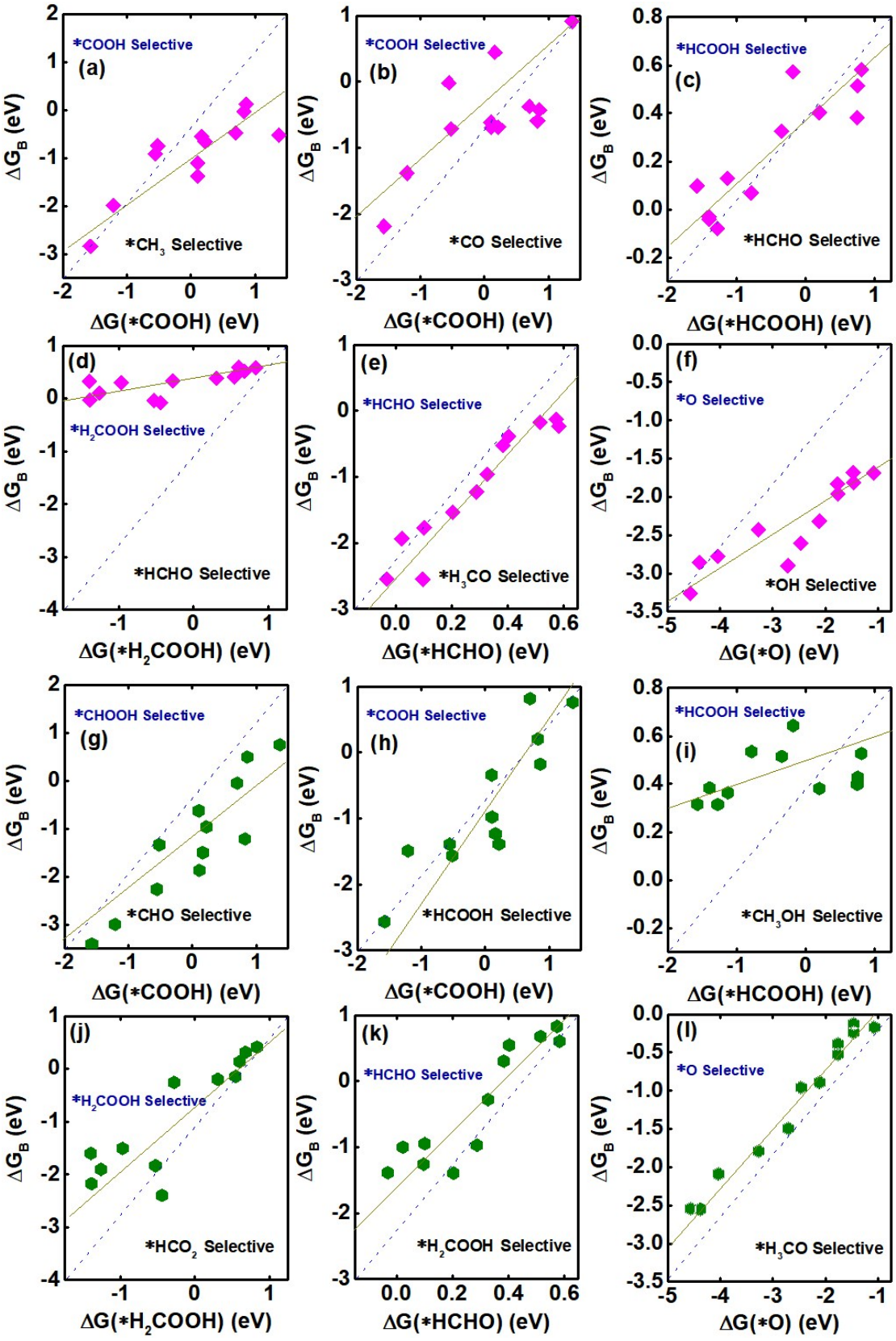
(a)
*COOH Selective
*CH3 Selective
ΔGB (eV)
ΔG(*COOH) (eV)
(b)
*COOH Selective
*CO Selective
ΔGB (eV)
ΔG(*COOH) (eV)
(c)
*HCOOH Selective
*HCHO Selective
ΔGB (eV)
ΔG(*HCOOH) (eV)
(d)
*H2COOH Selective
*HCHO Selective
ΔGB (eV)
ΔG(*H2COOH) (eV)
(e)
*HCHO Selective
*H3CO Selective
ΔGB (eV)
ΔG(*HCHO) (eV)
(f)
*O Selective
*OH Selective
ΔGB (eV)
ΔG(*O) (eV)
(g)
*CHOOH Selective
*CHO Selective
ΔGB (eV)
ΔG(*COOH) (eV)
(h)
*COOH Selective
*HCOOH Selective
ΔGB (eV)
ΔG(*COOH) (eV)
(i)
*HCOOH Selective
*CH3OH Selective
ΔGB (eV)
ΔG(*HCOOH) (eV)
(j)
*H2COOH Selective
*HCO2 Selective
ΔGB (eV)
ΔG(*H2COOH) (eV)
(k)
*HCHO Selective
*H2COOH Selective
ΔGB (eV)
ΔG(*HCHO) (eV)
(l)
*O Selective
*H3CO Selective
ΔGB (eV)
ΔG(*O) (eV)

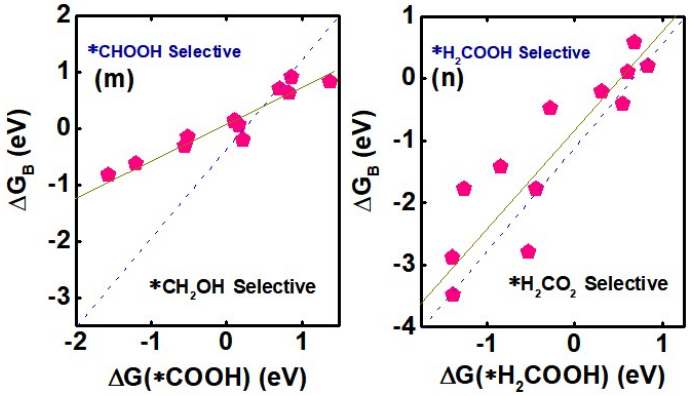

Figure. S3 Gibbs free energy changes (ΔG) linear relation for (a) the protonation step of COOH vs.CH_3, (b) COOH vs. CO, and (c) HCOOH formation vs. HCHO formation (d) H_2COOH vs. HCHO (e) HCHO vs. H_3CO (f) O vs. OH (g) COOH vs. CHO (h) COOH vs. HCOOH (i) HCOOH vs. CH_3OH (j) H_2COOH vs. HCO_2 (k) HCHO vs. H_2COOH (l) O vs. H_3CO (m) COOH vs. H_2COH (n) H_2COH vs. H_2CO_2 formation on MXene. Data points of M_3C_2 MXene below the dashed diagonal line are expected to be more selective towards upper than below, at U = 0V (vs.RHE).

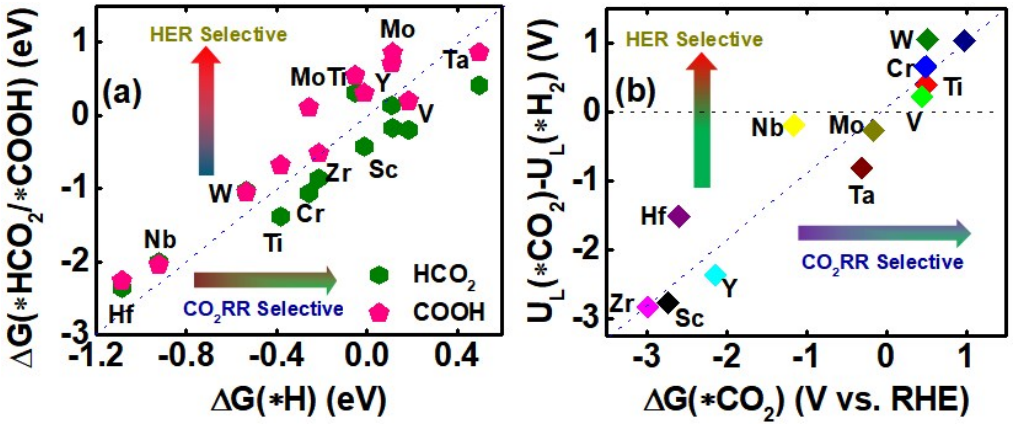

Figure. S4 Gibbs free energy changes (ΔG) for (a) the protonation step of CO_2RR (HCO_2 and COOH) vs. HER, (b) the protonation step of CO_2RR vs. HER selective towards. Data points of M_3C_2 MXene below the dashed diagonal line are expected to be more selective towards CO_2RR than HER, more selective towards *HCO_2 than *COOH formation, and more selective towards CO_2RR than HER formation at U = 0 V (vs. RHE).

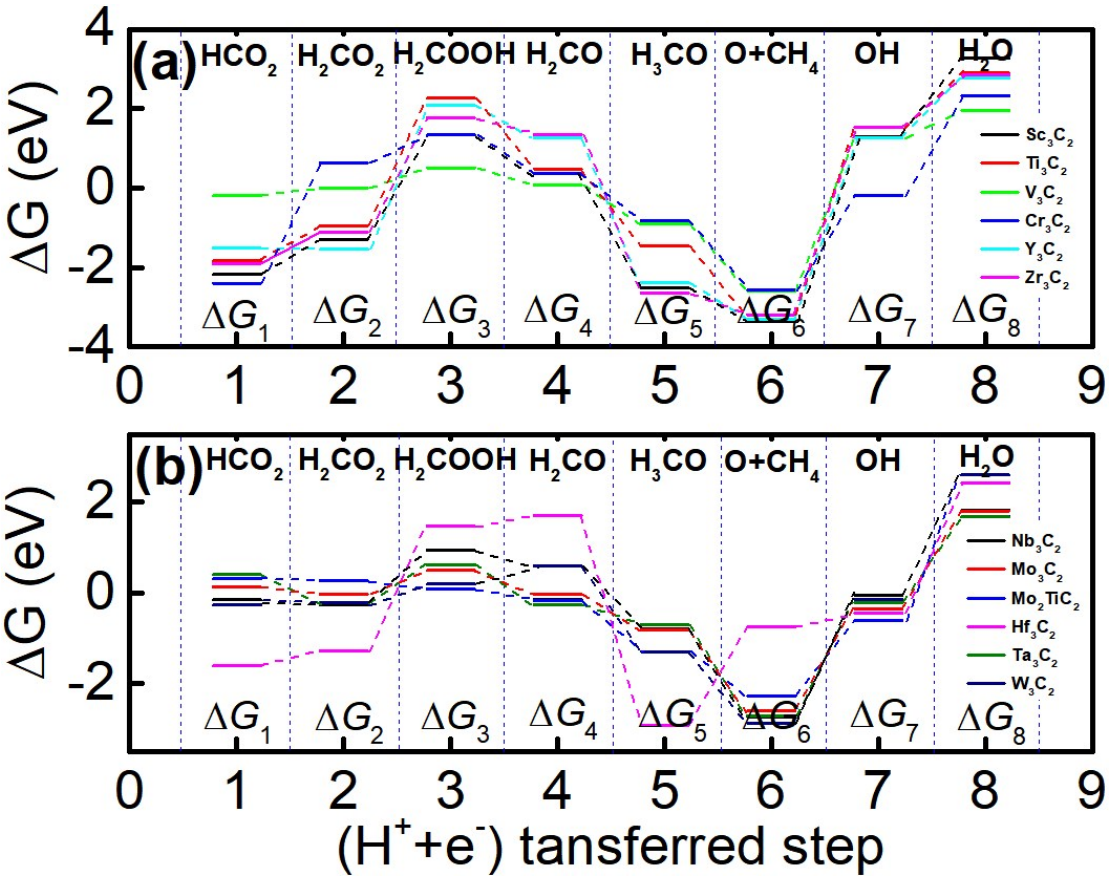

Figure. S6 Reaction gibbs free energy profiles for CO_2 reduction reactions along the the lowest energy pathway by using the relation limiting potential (U_L) on M_3C_2 type MXene (a) M =Sc, Ti, V, Cr, Y, and Zr (b) M =Nb, Mo, Mo_2Ti, Hf, Ta, Zr and W at 0 V (vs. RHE).

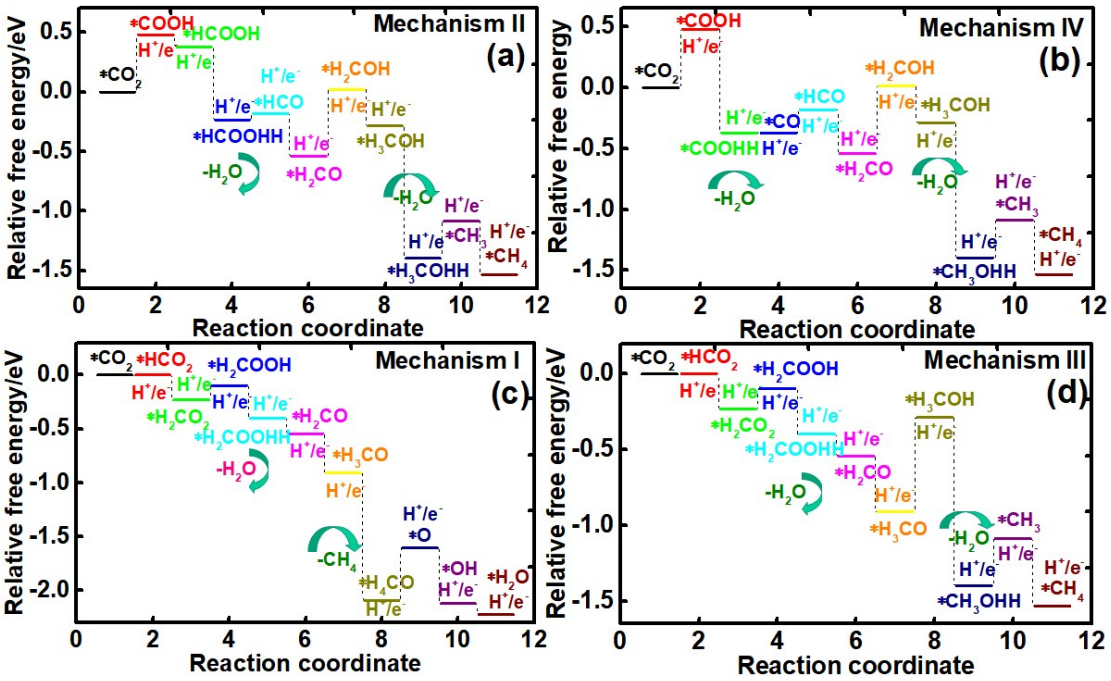

Figure.S7 Free energy diagrams of the overall CO_2RR pathway for all reaction pathways on Mo_3C_2 at 0 V vs. the RHE. (a) Pathway 1 (b) Pathway 2 (c) Pathway3 (d) Pathway 4.

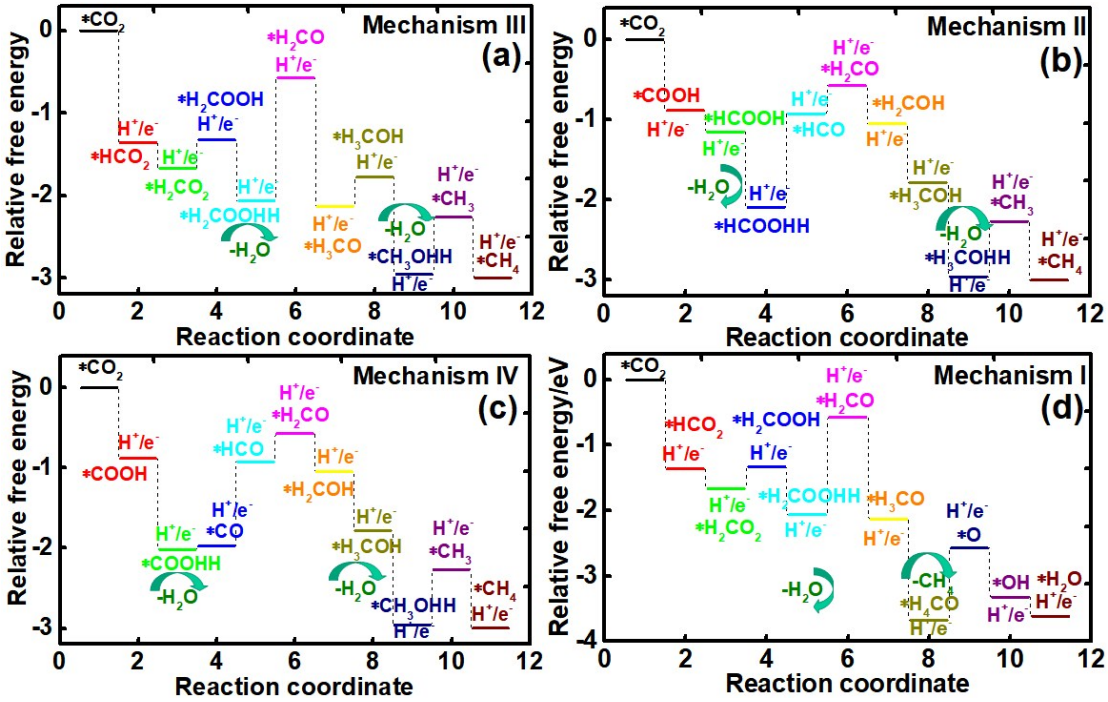

Figure. S8 Free energy diagrams of the overall CO_2RR pathway for all reaction pathways on Mo_2TiC_2 at 0 V vs. the RHE. (a) Pathway 1 (b) Pathway 2 (c) Pathway 3 (d) Pathway 4.

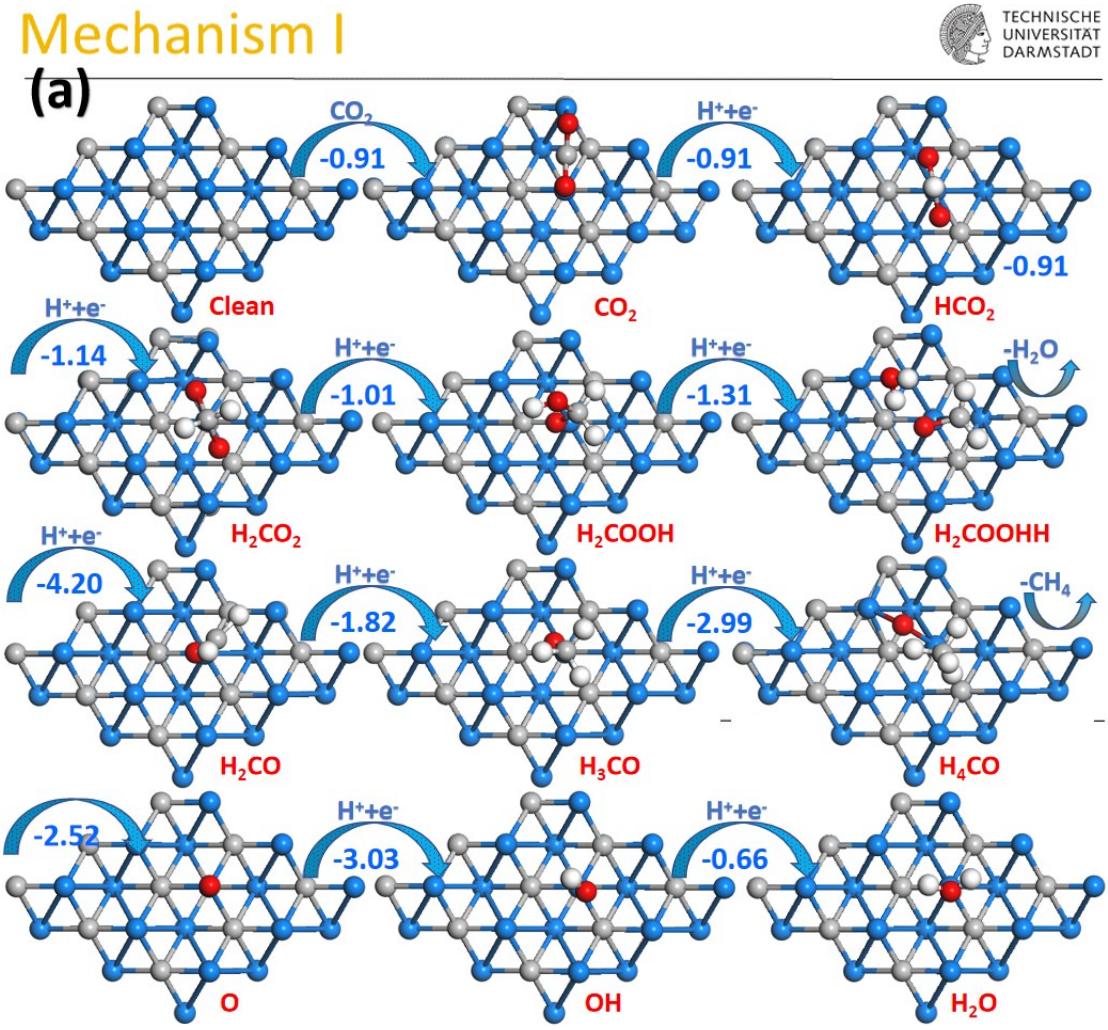

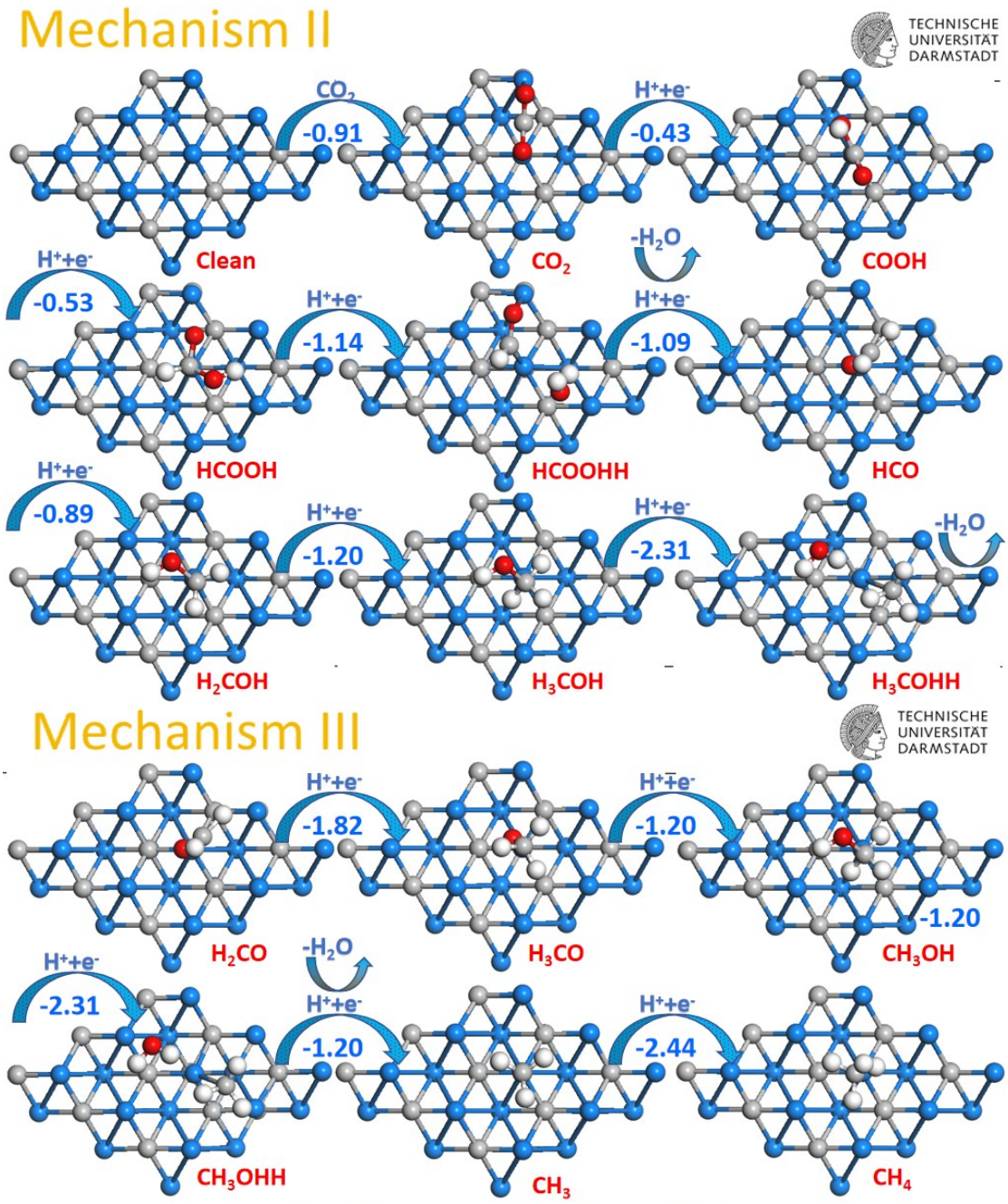

Continue mechanism I (6)

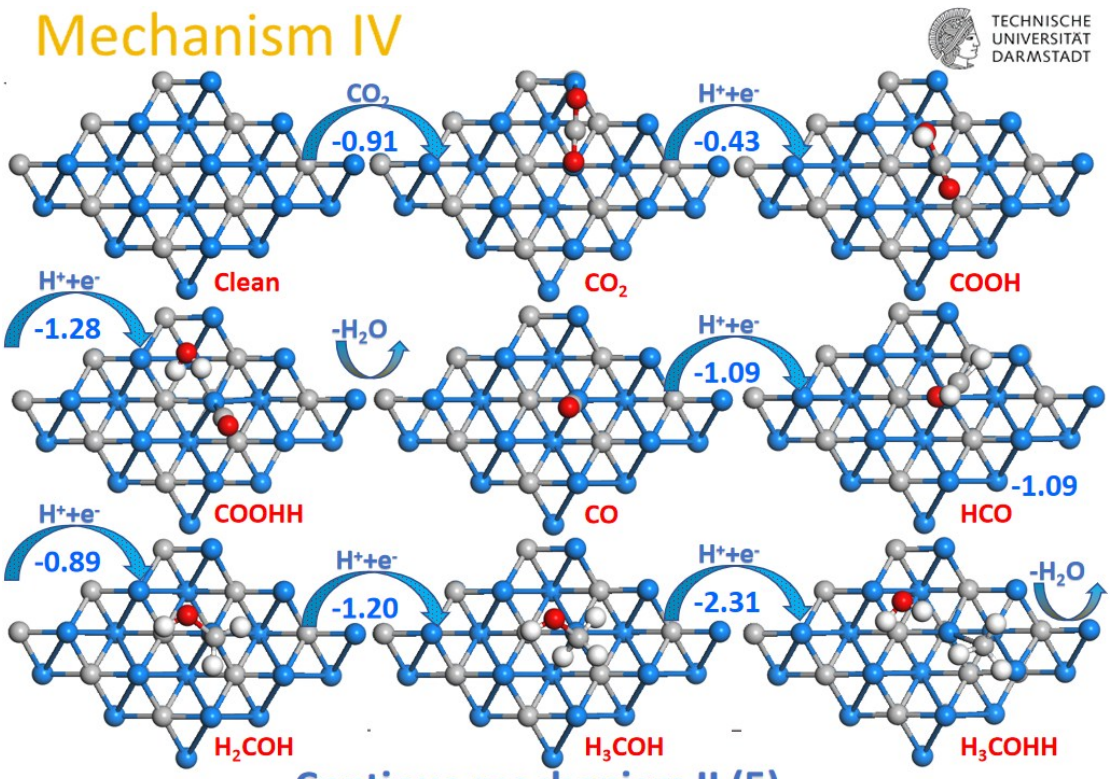

Continue mechanism II (5)

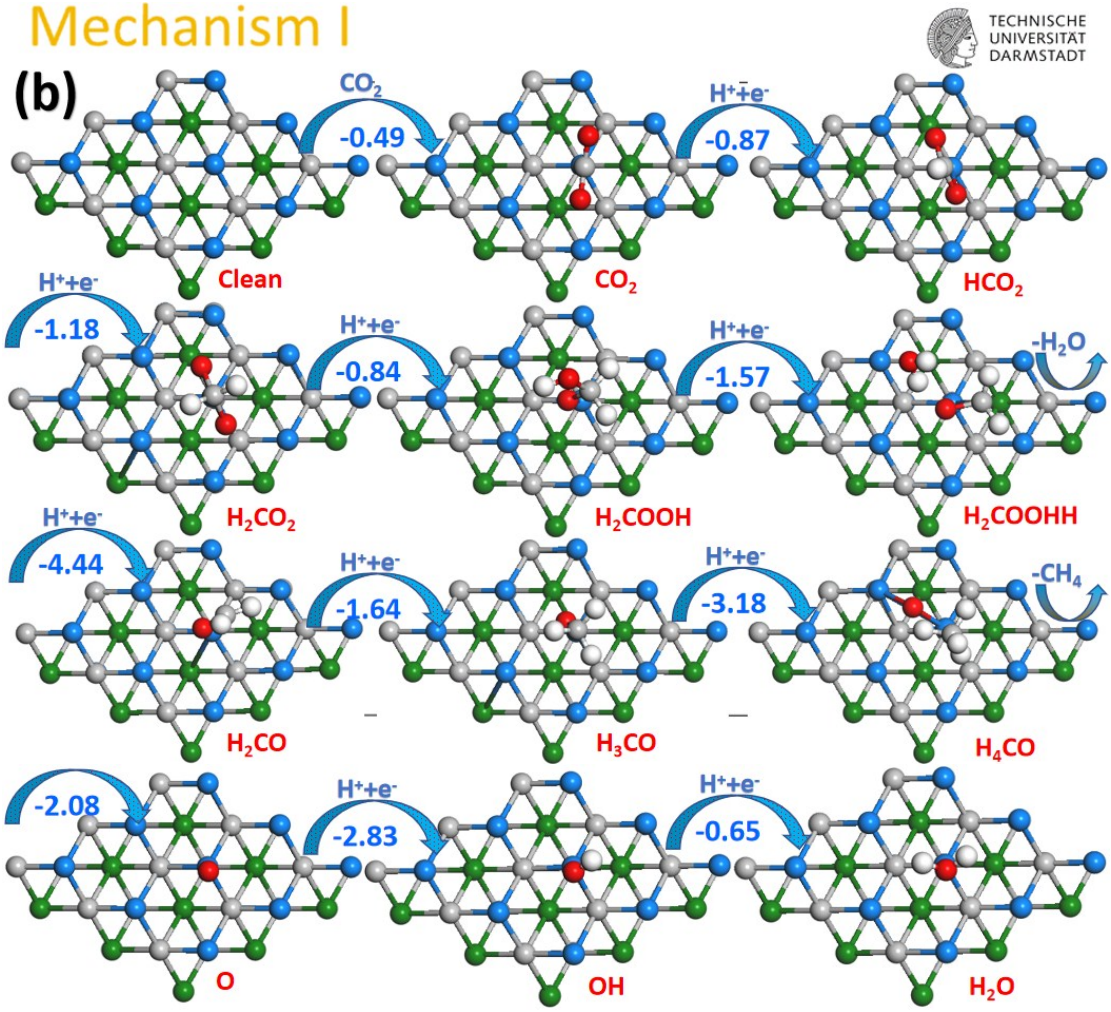

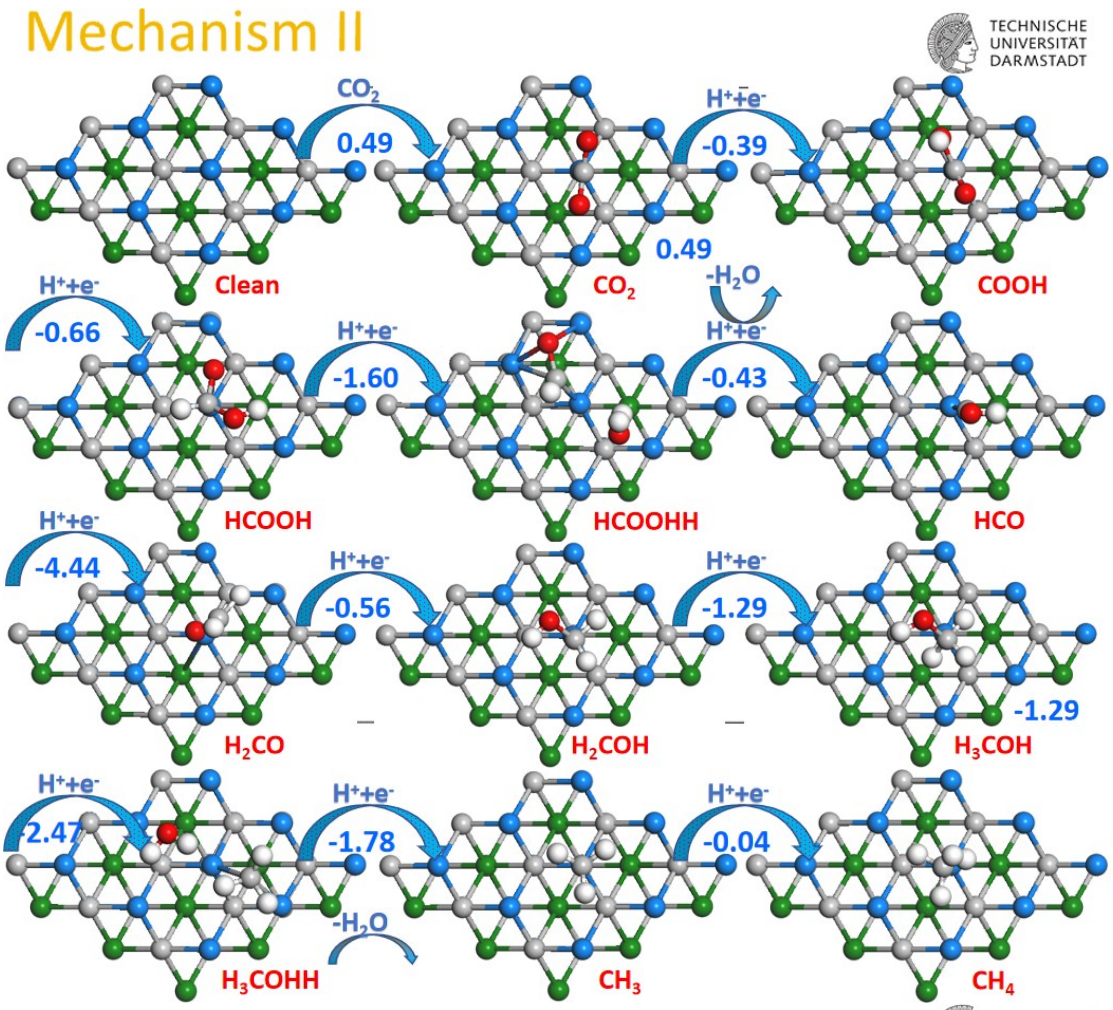

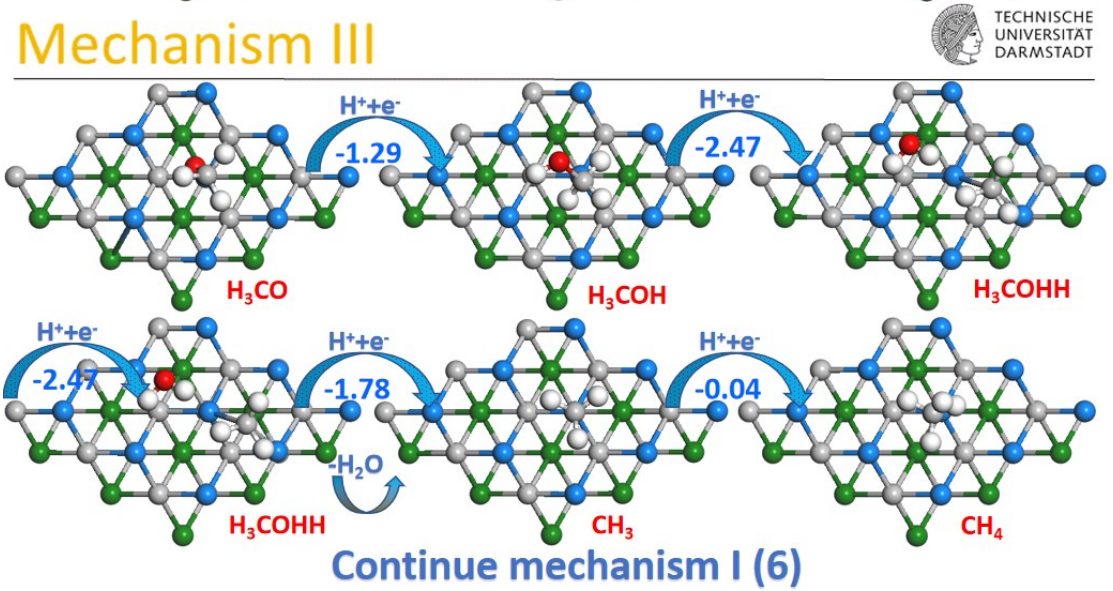

Continue mechanism I (6)

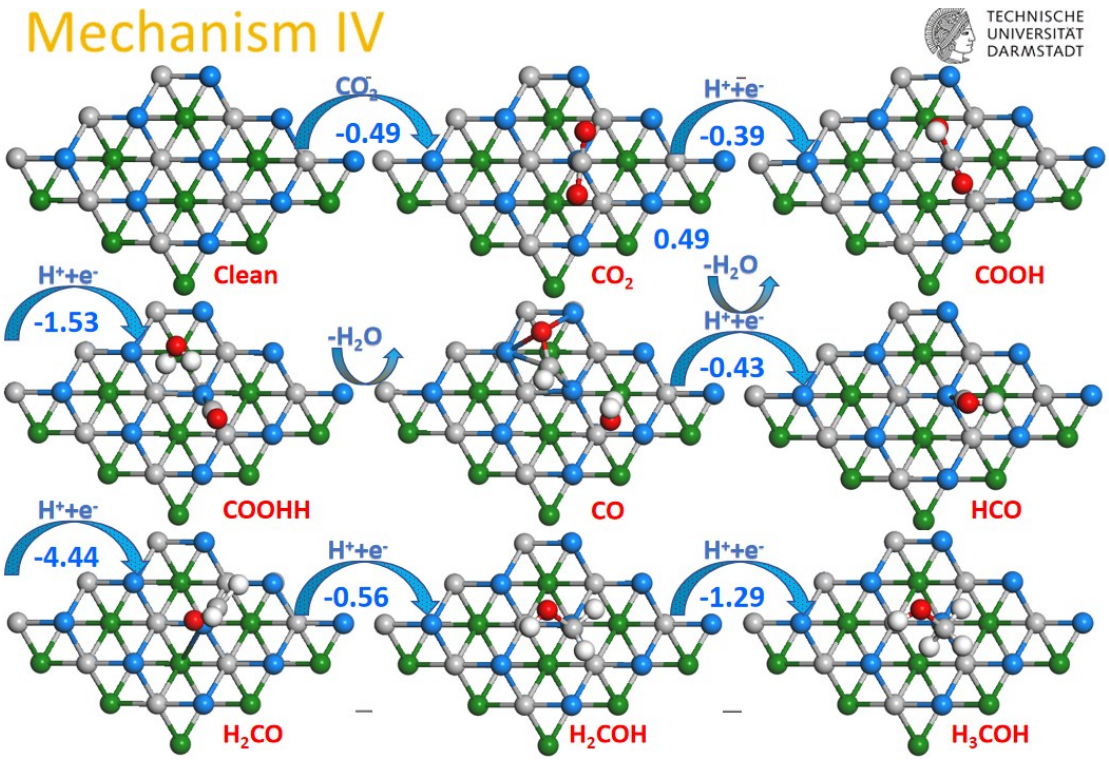

Figure. S9 Top view of energy path followed for the CO_2 conversion mechanism into CH_4 and H_2O catalyzed by MXene. the blue numbers represent the energy required to carry out a reaction step (in eV). (a) Mo_3C_2 (b) Mo_2TiC_2.

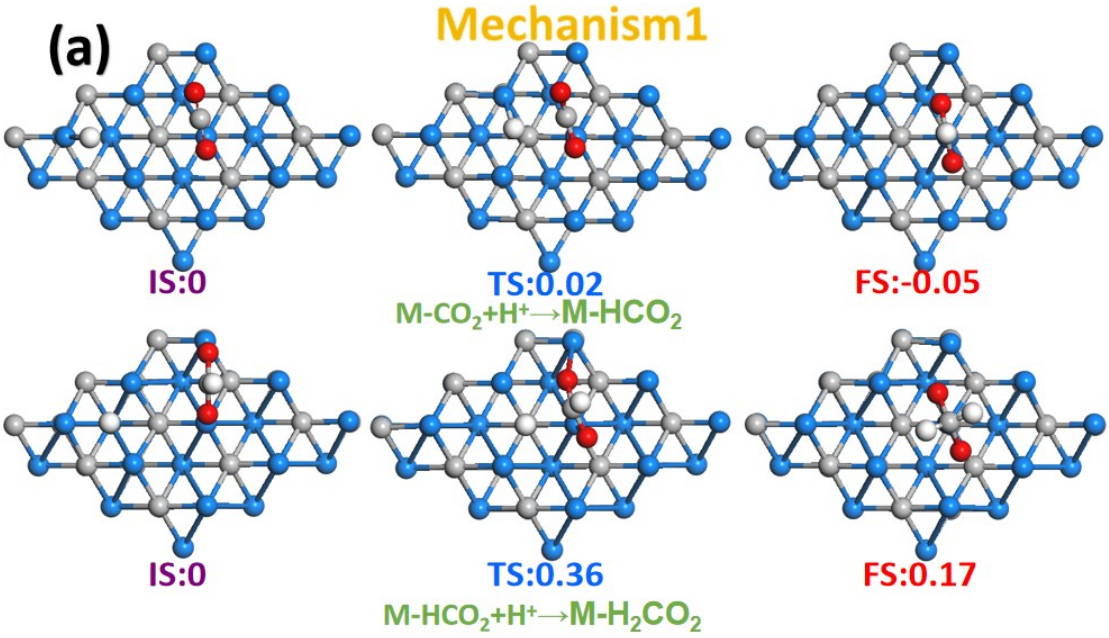

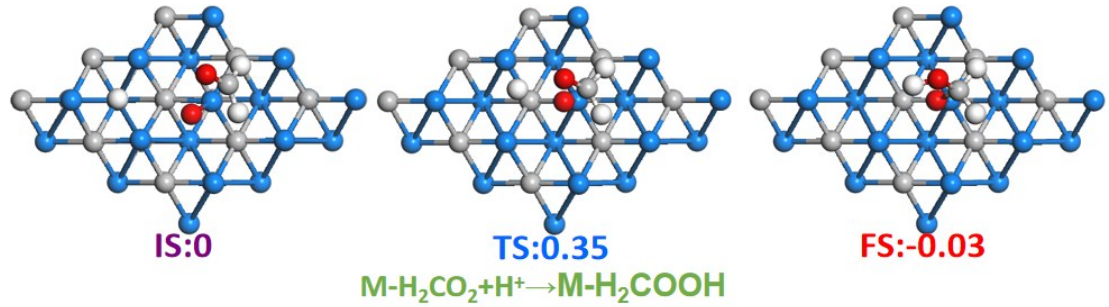

$M\text{-}H_2CO_2+H^+ \rightarrow M\text{-}H_2COOH$

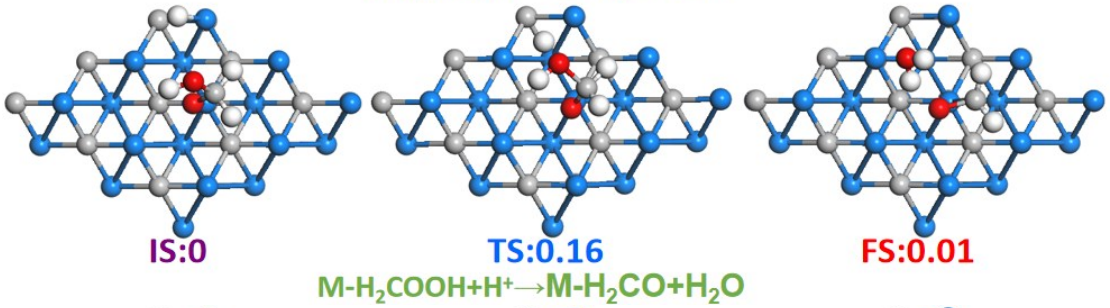

$M\text{-}H_2COOH+H^+ \rightarrow M\text{-}H_2CO+H_2O$

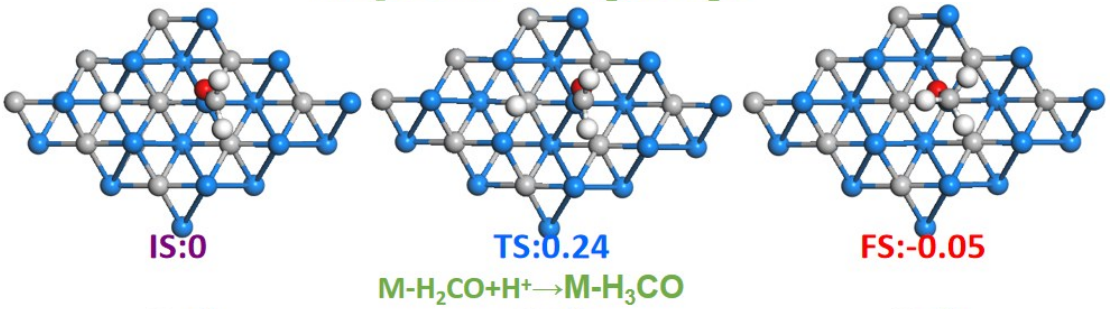

$M\text{-}H_2CO+H^+ \rightarrow M\text{-}H_3CO$

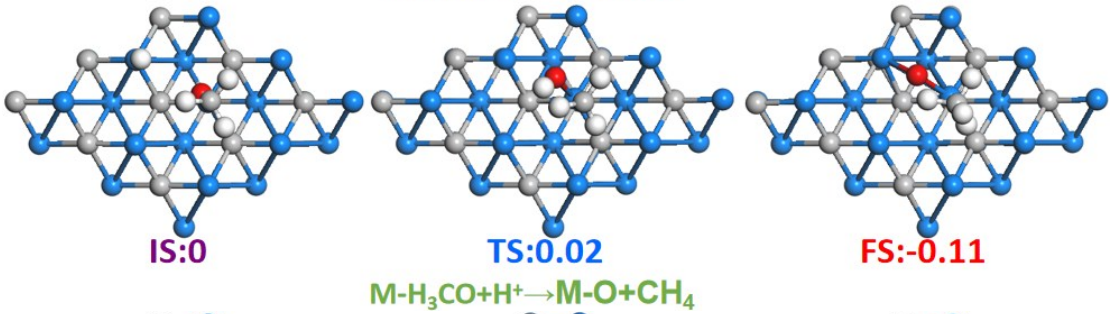

$M\text{-}H_3CO+H^+ \rightarrow M\text{-}O+CH_4$

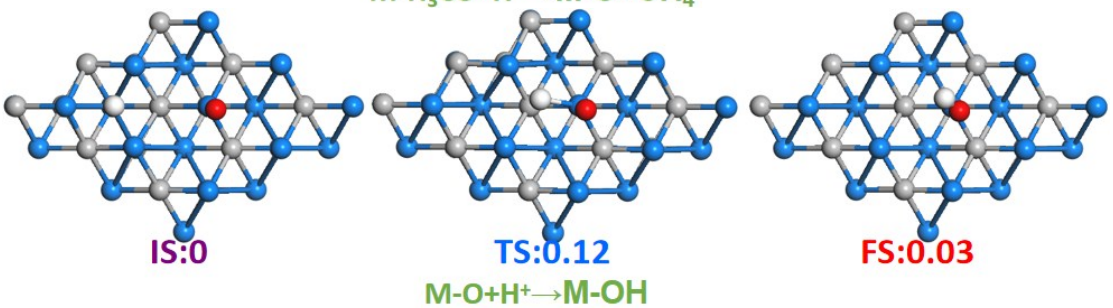

$M\text{-}O+H^+ \rightarrow M\text{-}OH$

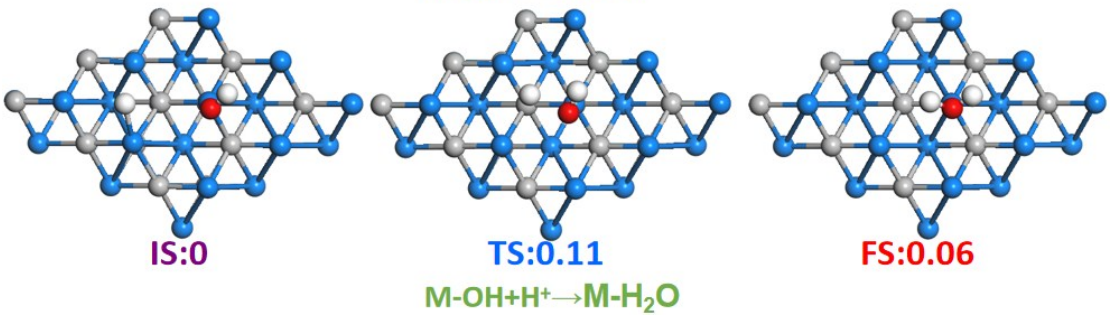

$M\text{-}OH+H^+ \rightarrow M\text{-}H_2O$

Figure. S10 Top view of various possible reaction pathways for CO_2RR on the (a) Mo_3C_2 (b) Mo_2TiC_2 MXene monolayer, respectively. Here, the transition states (TS) are marked and the corresponding reaction barrier (TS) and reaction energy (Δ E), the change in the total energies between products and reactants are also presented, the activation energies and reaction energies (in units of eV) are given in blue and red numbers, respectively.

Elementary reaction mechanism

Detailed calculations

Elementary reaction steps

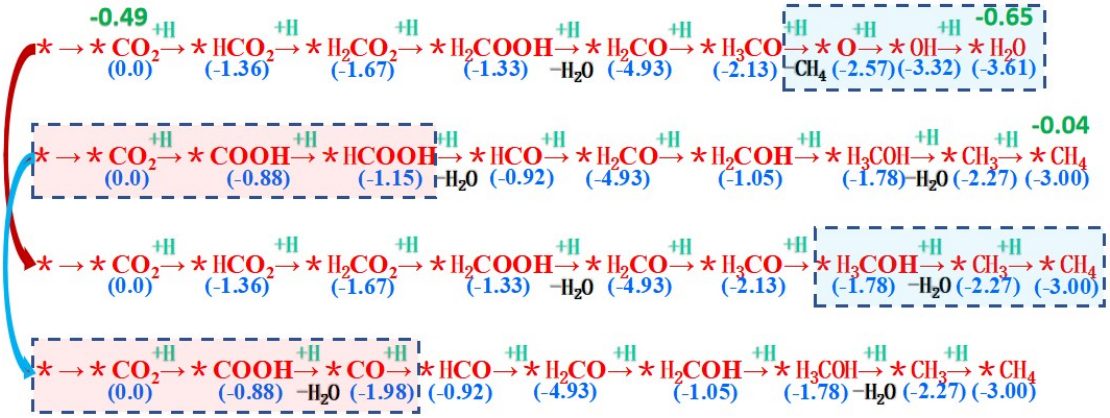

Formation energy

(1) M+CO_2→M-CO_2

$$\Delta E = E_{M-CO_2} - E_M - E_{CO_2}$$

(2) M+CO_2+1/2H_2+e⁻→M-HCO_2

$$\Delta E = E_{M-HCO_2} - E_M - E_{CO_2} - 1/2E_{H_2}$$

(3) M+CO_2+H_2+2e⁻→M-H_2CO_2

$$\Delta E = E_{M-H_2CO_2} - E_M - E_{CO_2} - E_{H_2}$$

(4) M+CO_2+3/2H_2+3e⁻→M-H_2COOH

$$\Delta E = E_{M-H_2COOH} - E_M - E_{CO_2} - 3/2E_{H_2}$$

(5) M+CO_2+2H_2+4e⁻→M-H_2CO+H_2O

$$\Delta E = E_{M-H_2CO} + E_{H_2O} - E_M - E_{CO_2} - 2E_{H_2}$$

(6) M+CO_2+5/2H_2+5e⁻→M-H_3CO+H_2O

$$\Delta E = E_{M-H_3CO} + E_{H_2O} - E_M - E_{CO_2} - 5/2E_{H_2}$$

(7) M+CO_2+3H_2+6e⁻→M-O+H_2O+CH_4

$$\Delta E = E_{M-O} + E_{H_2O} + E_{CH_4} - E_M - E_{CO_2} - 3E_{H_2}$$

(8) M+CO_2+7/2H_2+7e⁻→M-OH+H_2O+CH_4

$$\Delta E = E_{M-OH} + E_{H_2O} + E_{CH_4} - E_M - E_{CO_2} - 7/2E_{H_2}$$

(9) M+CO_2+4H_2+8e⁻→M-CH_4+2H_2O

$$\Delta E = E_{M-CH_4} + 2E_{H_2O} - E_M - E_{CO_2} - 4E_{H_2}$$

Formation energy

(1) M+CO_2→M-CO_2

$$\Delta E = E_{M-CO_2} - E_M - E_{CO_2}$$

(2) M+CO_2+1/2H_2+e⁻→M-COOH

$$\Delta E = E_{M-COOH} - E_M - E_{CO_2} - 1/2E_{H_2}$$

(3) M+CO_2+H_2+2e⁻→M-HCOOH

$$\Delta E = E_{M-HCOOH} - E_M - E_{CO_2} - E_{H_2}$$

(4) M+CO_2+3/2H_2+3e⁻→M-HCO+H_2O

$$\Delta E = E_{M-HCO} + E_{H_2O} - E_M - E_{CO_2} - 3/2E_{H_2}$$

(5) M+CO_2+2H_2+4e⁻→M-H_2CO+H_2O

$$\Delta E = E_{M-H_2CO} + E_{H_2O} - E_M - E_{CO_2} - 2E_{H_2}$$

(6) M+CO_2+5/2H_2+5e⁻→M-H_2COH+H_2O

$$\Delta E = E_{M-H_2COH} + E_{H_2O} - E_M - E_{CO_2} - 5/2E_{H_2}$$

(7) M+CO_2+3H_2+6e⁻→M-CH_3OH+H_2O

$$\Delta E = E_{M-CH_3OH} + E_{H_2O} - E_M - E_{CO_2} - 3E_{H_2}$$

(8) M+CO_2+7/2H_2+7e⁻→M-CH_3+2H_2O

$$\Delta E = E_{M-CH_3} + 2E_{H_2O} - E_M - E_{CO_2} - 7/2E_{H_2}$$

(9) M+CO_2+4H_2+8e⁻→M-CH_4+2H_2O

$$\Delta E = E_{M-CH_4} + 2E_{H_2O} - E_M - E_{CO_2} - 4E_{H_2}$$

Formation energy

Continue mechanism I (6)

(6) M+CO_2+5/2H_2+5e$^-$→M-H_3CO+H_2O

$$\Delta E = E_{M-H_3CO} + E_{H_2O} - E_M - E_{CO_2} - 5/2E_{H_2}$$

(7) M+CO_2+3H_2+6e$^-$→M-H_3COH+H_2O

$$\Delta E = E_{M-H_3COH} + E_{H_2O} - E_M - E_{CO_2} - 3E_{H_2}$$

(1) M+CO_2+1/2H_2+e$^-$→M-COOH

$$\Delta E = E_{M-COOH} - E_M - E_{CO_2} - 1/2E_{H_2}$$

(2) M+CO_2+H_2+2e$^-$→M-CO+H_2O

$$\Delta E = E_{M-CO} + E_{H_2O} - E_M - E_{CO_2} - E_{H_2}$$

Continue mechanism II (5)

(8) M+CO_2+7/2H_2+7e$^-$→M-H_3C+2H_2O

$$\Delta E = E_{M-H_3C} + 2E_{H_2O} - E_M - E_{CO_2} - 7/2E_{H_2}$$

(9) M+CO_2+4H_2+8e$^-$→M-H_4C+2H_2O

$$\Delta E = E_{M-CH_4} + 2E_{H_2O} - E_M - E_{CO_2} - 4E_{H_2}$$

(3) M+CO_2+3/2H_2+3e$^-$→M-HCO+H_2O

$$\Delta E = E_{M-HCO} + E_{H_2O} - E_M - E_{CO_2} - 3/2E_{H_2}$$

(4) M+CO_2+2H_2+4e$^-$→M-H_2CO+H_2O

$$\Delta E = E_{M-H_2CO} + E_{H_2O} - E_M - E_{CO_2} - 2E_{H_2}$$

Mechanism I

(1) M+CO_2+H$^+$+e$^-$→M-HCO_2

$$\Delta G_1 = \Delta G_{M-HCO_2} + U_1^0$$

(2) M-HCO_2+H$^+$+e$^-$→M-H_2CO_2

$$\Delta G_2 = \Delta G_{M-H_2CO_2} - \Delta G_{M-HCO_2} + U_2^0$$

(3) M-H_2CO_2+H$^+$+e$^-$→M-H_2COOH

$$\Delta G_3 = \Delta G_{M-H_2COOH} - \Delta G_{M-H_2CO_2} + U_3^0$$

(4) M-H_2COOH+H$^+$+e$^-$→M-H_2CO+H_2O

$$\Delta G_4 = \Delta G_{M-H_2CO} + \Delta G_{H_2O} - \Delta G_{M-H_2COOH} + U_4^0$$

(5) M-H_2CO+H$^+$+e$^-$→M-H_3CO

$$\Delta G_5 = \Delta G_{M-H_3CO} - \Delta G_{M-H_2CO_2} + U_5^0$$

(6) M-H_3CO+H$^+$+e$^-$→M-O+CH_4

$$\Delta G_6 = \Delta G_{M-O} + \Delta G_{CH_4} - \Delta G_{M-H_3CO} + U_6^0$$

(7) M-O+H$^+$+e$^-$→M-OH

$$\Delta G_7 = \Delta G_{M-OH} - \Delta G_{M-O} + U_7^0$$

(8) M-OH+H$^+$+e$^-$→M-H_2O

$$\Delta G_8 = \Delta G_{H_2O} - \Delta G_{M-OH} + U_8^0$$

Total reaction:CO_2+8H$^+$+8e$^-$→CH_4+2H_2O

$\Delta G_1+\Delta G_2+\Delta G_3+\Delta G_4+\Delta G_5+\Delta G_6+\Delta G_7+\Delta G_8$=-5.47

Mechanism II

(1) M+CO_2+H$^+$+e$^-$→M-COOH

$$\Delta G_1 = \Delta G_{M-COOH} + U_1^0$$

(2) M-COOH+H$^+$+e$^-$→M-HCOOH

$$\Delta G_2 = \Delta G_{M-HCOOH} - \Delta G_{M-COOH} + U_2^0$$

(3) M-HCOOH+H$^+$+e$^-$→M-HCO+H_2O

$$\Delta G_3 = \Delta G_{M-HCO} + \Delta G_{H_2O} - \Delta G_{M-HCOOH} + U_3^0$$

(4) M-HCO+H$^+$+e$^-$→M-H_2CO

$$\Delta G_4 = \Delta G_{M-H_2CO} - \Delta G_{M-HCO} + U_4^0$$

(5) M-H_2CO+H$^+$+e$^-$→M-H_2COH

$$\Delta G_5 = \Delta G_{M-H_2COH} - \Delta G_{M-H_2CO} + U_5^0$$

(6) M-H_2COH+H$^+$+e$^-$→M-H_3COH

$$\Delta G_6 = \Delta G_{M-H_3COH} - \Delta G_{M-H_2COH} + U_6^0$$

(7) M-H_3COH+H$^+$+e$^-$→M-CH_3 +H_2O

$$\Delta G_7 = \Delta G_{M-CH_3} + \Delta G_{H_2O} - \Delta G_{M-H_3COH} + U_7^0$$

(8) M-CH_3+H$^+$+e$^-$→M-CH_4

$$\Delta G_8 = \Delta G_{M-CH_4} - \Delta G_{M-CH_3} + U_8^0$$

Total reaction:CO_2+8H$^+$+8e$^-$→CH_4+2H_2O

$\Delta G_1+\Delta G_2+\Delta G_3+\Delta G_4+\Delta G_5+\Delta G_6+\Delta G_7+\Delta G_8$=-5.47

Mechanism III

(1) $M+CO_2+H^++e^-\rightarrow M\text{-}HCO_2$

$$\Delta G_1 = \Delta G_{M-HCO_2} + U_1^0$$

(2) $M\text{-}HCO_2+H^++e^-\rightarrow M\text{-}H_2CO_2$

$$\Delta G_2 = \Delta G_{M-H_2CO_2} - \Delta G_{M-HCO_2} + U_2^0$$

(3) $M\text{-}H_2CO_2+H^++e^-\rightarrow M\text{-}H_2COOH$

$$\Delta G_3 = \Delta G_{M-H_2COOH} - \Delta G_{M-H_2CO_2} + U_3^0$$

(4) $M\text{-}H_2COOH+H^++e^-\rightarrow M\text{-}H_2CO+H_2O$

$$\Delta G_4 = \Delta G_{M-H_2CO} + \Delta G_{H_2O} - \Delta G_{M-H_2COOH} + U_4^0$$

(5) $M\text{-}H_2CO+H^++e^-\rightarrow M\text{-}H_3CO$

$$\Delta G_5 = \Delta G_{M-H_3CO} - \Delta G_{M-H_2CO_2} + U_5^0$$

(6) $M\text{-}H_3CO+H^++e^-\rightarrow M\text{-}CH_3OH$

$$\Delta G_6 = \Delta G_{M-O} + \Delta G_{CH_4} - \Delta G_{M-H_3CO} + U_6^0$$

(7) $M\text{-}CH_3OH+H^++e^-\rightarrow M\text{-}CH_3+H_2O$

$$\Delta G_7 = \Delta G_{M-CH_3} + \Delta G_{H_2O} - \Delta G_{M-CH_3OH} + U_7^0$$

(8) $M\text{-}CH_3+H^++e^-\rightarrow M\text{-}CH_4$

$$\Delta G_8 = \Delta G_{CH_4} - \Delta G_{M-CH_3} + U_8^0$$

Total reaction: $CO_2+8H^++8e^-\rightarrow CH_4+2H_2O$

$\Delta G_1+\Delta G_2+\Delta G_3+\Delta G_4+\Delta G_5+\Delta G_6+\Delta G_7+\Delta G_8=-5.47$

Mechanism IV

(1) $M+CO_2+H^++e^-\rightarrow M\text{-}COOH$

$$\Delta G_1 = \Delta G_{M-COOH} + U_1^0$$

(2) $M\text{-}COOH+H^++e^-\rightarrow M\text{-}HCOOH$

$$\Delta G_2 = \Delta G_{M-HCOOH} - \Delta G_{M-COOH} + U_2^0$$

(3) $M\text{-}HCOOH+H^++e^-\rightarrow M\text{-}HCO+H_2O$

$$\Delta G_3 = \Delta G_{M-HCO} + \Delta G_{H_2O} - \Delta G_{M-HCOOH} + U_3^0$$

(4) $M\text{-}HCO+H^++e^-\rightarrow M\text{-}H_2CO$

$$\Delta G_4 = \Delta G_{M-H_2CO} - \Delta G_{M-HCO} + U_4^0$$

(5) $M\text{-}H_2CO+H^++e^-\rightarrow M\text{-}H_2COH$

$$\Delta G_5 = \Delta G_{M-H_2COH} - \Delta G_{M-H_2CO} + U_5^0$$

(6) $M\text{-}H_2COH+H^++e^-\rightarrow M\text{-}H_3COH$

$$\Delta G_6 = \Delta G_{M-H_3COH} - \Delta G_{M-H_2COH} + U_6^0$$

(7) $M\text{-}H_3COH+H^++e^-\rightarrow M\text{-}CH_3+H_2O$

$$\Delta G_7 = \Delta G_{M-CH_3} + \Delta G_{H_2O} - \Delta G_{M-H_3COH} + U_7^0$$

(8) $M\text{-}CH_3+H^++e^-\rightarrow M\text{-}CH_4$

$$\Delta G_8 = \Delta G_{M-CH_4} - \Delta G_{M-CH_3} + U_8^0$$

Total reaction: $CO_2+8H^++8e^-\rightarrow CH_4+2H_2O$

$\Delta G_1+\Delta G_2+\Delta G_3+\Delta G_4+\Delta G_5+\Delta G_6+\Delta G_7+\Delta G_8=-5.47$

References

1. Greeley, J.; Nørskov, J. K., Electrochemical dissolution of surface alloys in acids: Thermodynamic trends from first-principles calculations. Electrochimica Acta 2007, 52, 5829-5836.

2. Henkelman, G.; Arnaldsson, A.; Jónsson, H., A fast and robust algorithm for Bader decomposition of charge density. Comput. Mater. Sci. 2006, 36, 354-360.

3. Nørskov, J. K.; Rossmeisl, J.; Logadottir, A.; Lindqvist, L.; Kitchin, J. R.; Bligaard, T.; Jónsson, H., Origin of the Overpotential for Oxygen Reduction at a Fuel-Cell Cathode. J. Phys. Chem. B 2004, 108, 17886-17892.

4. Peterson, A. A.; Abild-Pedersen, F.; Studt, F.; Rossmeisl, J.; Nørskov, J. K., How copper catalyzes the electroreduction of carbon dioxide into hydrocarbon fuels. Energy Environ. Sci. 2010, 3, 1311-1315.

5. He, B. L.; Shen, J. S.; Tian, Z. X., Iron-embedded C_2N monolayer: a promising low-cost and high-activity single-atom catalyst for CO oxidation. Phys. Chem. Chem. Phys. 2016, 18, 24261-24269.